Supplementary Material

Fig. S1. Comparison of CDOM absorption spectra before and after irradiation. A): Sta. 170, surface (1-h irradiation); B): Sta. 670, surface (1.5-h irradiation); C): Sta. 135, DCM (3-h irradiation, the longest irradiation in this study for short cutoff filters). For unfiltered samples, they were filtered with 0.2-μm Nylon syringe filters after irradiation. Note some lines are almost completely overlapped.

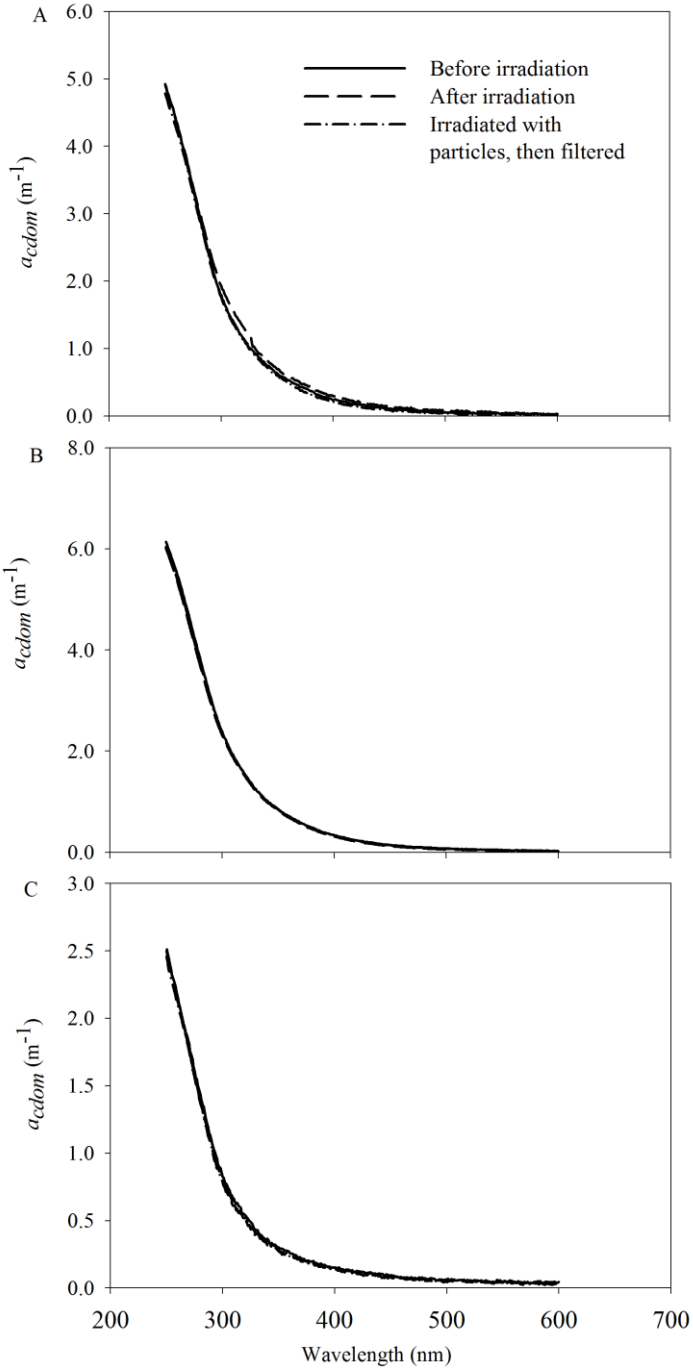

Monte Carlo Simulation. The quantum absorbed (Q_a) by an optically significant constituent inside a quartz cell irradiated from above by a collimated light beam[1] can be estimated using Eq. (3) in the paper (abbreviated as Eq. (3) herein), as long as the light scattering is negligible relative to the absorption. Filtered seawater with dissolved organic matter (DOM) meets this requirement, since both seawater and DOM have low scattering and CDOM absorption coefficient in short wavelengths is large (i.e. b:$a \sim 0$; b: scattering coefficient and a: absorption coefficient). Unfiltered seawater, however, may not meet this requirement, since scattering by particles can increase the path-length of some photons (i.e. path-length amplification, PA herein) but deflect some other photons out of the quartz cell in all directions (i.e. scattering loss, SL herein). Under this circumstance, Eq. (3) overestimates Q_a if SL > PA or underestimates Q_a if PA > SL. Here we assessed the effect of particle scattering on the quantity of photons absorbed using Monte Carlo (MC) simulations (SimulO software; Leymarie et al. 2010) and proposed a modification to Eq. (3) to account for the scattering effect.

MC was used to simulate the trajectories of collimated photons hitting a vertically placed cylindrical quartz cell (length: 114 mm, o.d.: 34 mm, wall thickness: 1.5mm, refractive index: 1.48) from above. The refractive index of pure seawater was set to be 1.34 and its inherent optical properties were taken from Morel (1974) and Buitelveld (1994). All photons scattered out of the cell's side wall were assumed to be totally absorbed by the black electric tape that wrapped the cell. The reflection from the bottom quartz window was ignored since it was in contact with a black plastic block. The particle phase function was given by the Fournier-Forand model (Fournier and Forand, 1994; Mobley et al., 2002) with a backscattering ratio of 2.2%. This backscattering ratio is within the range observed by Doxaran et al. (2012) in the study area.

Absorption and scattering coefficient values used in our simulations cover the large ranges encountered during the Malina cruise (a_t: 0.045–47.2 m^{-1}; b: 0.056–241.5 m^{-1}; b/a_t: 0.12–20.4). The total absorption (a_t, m^{-1}) coefficient is the sum of pure seawater, CDOM and particle absorption coefficients, whereas scattering coefficient (b, m^{-1}) is only the particle scattering coefficient. Scattering by pure water was neglected as it was several orders of magnitude lower than a_t or b. For each simulation (i.e. a given set of b and a_t). The SimulO software computed the number of photons absorbed within the water body, taking into account all scattering and reflection processes. Then, this number was compared to the number of absorbed photons calculated from Eq. (3) without accounting for the scattering effect.

For a given a_t, the ratio (R) of the number of absorbed photons calculated using Eq. (3) to that from the MC simulation is found to be linearly correlated to b:a_t within the range of 0 to 25 (Fig. S2):

$$R = S \times \left(\frac{b}{a_t}\right) + 1 \qquad \text{(S1)}$$

where S is the regressed slope. S increases with a_t in a manner of exponential rise to maximum (Fig. S3) as expressed by Eq. (S2):

$$S = 0.0539(1 - e^{-0.191 a_t}) \qquad \text{(S2)}$$

[1] Justification of collimated light reaching the sample's surface in the quartz cell can be found in the Support Information of the study by Zhang et al. (2006). This is also confirmed by a direct comparison between the multispectral irradiation system as adopted in our study and a monochromatic system in the measurement of CO AQY (Ziolkowski and Miller, 2007).

R for our Malina samples can thus be calculated from Eqs. (S1) and (S2) with known values of a_t and b; a_t is from our own study while b is from the study of Doxaran et al. (2012). Fig. S4 shows R as a function of wavelength. The scattering effect (i.e. R–1) was ≤0.3% in the CB and ≤1.9% on the MS, including two outermost stations along the SGTs (Sta. 392 and 691). Samples from the remaining SGT stations had larger a_t values (1.00–10.45 m^{-1} at 412 nm) and higher scattering to absorption ratios (2.8–9.8 at 412 nm). The scattering effect for these stations ranged from 2.0% to 27.8%, depending on sampling location and wavelength. The effect was positive, indicating SL was larger than PA.

Fig. S2. Ratio (R) of the number of absorbed photons calculated using Eq. (3) to that from the MC simulation at various b:a_t and a_t values.

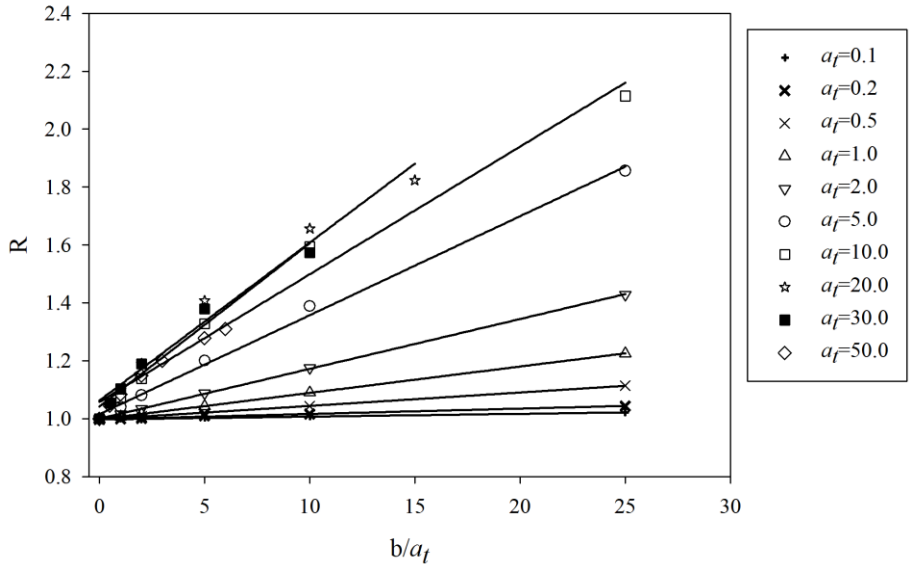

Fig. S3. Regressed slope (S) in Fig. S2 as a function of a_t.

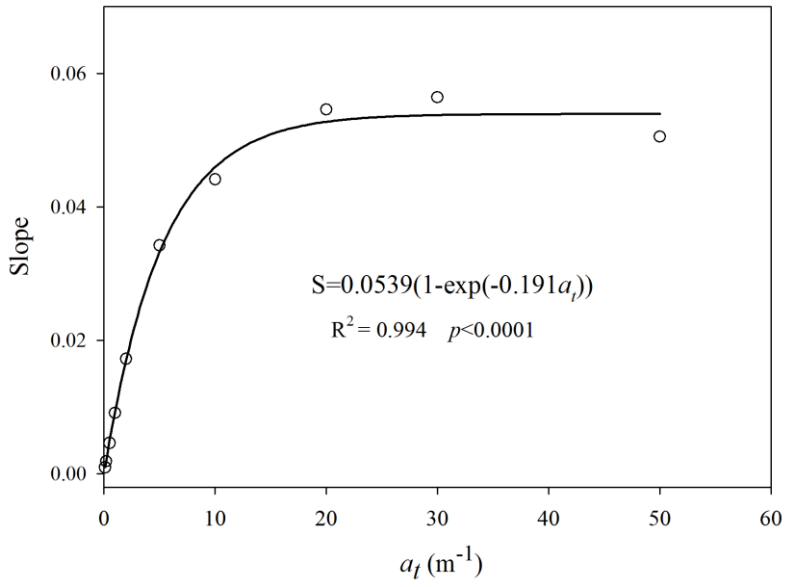

Fig. S4. R as a function of wavelength for Malina samples. Stations with $R \geq 2\%$ are presented individually while stations with $R < 2\%$ are presented by mean values. Mean value for the MS include two outermost stations (Sta. 392 and 691) along the salinity gradient transects.

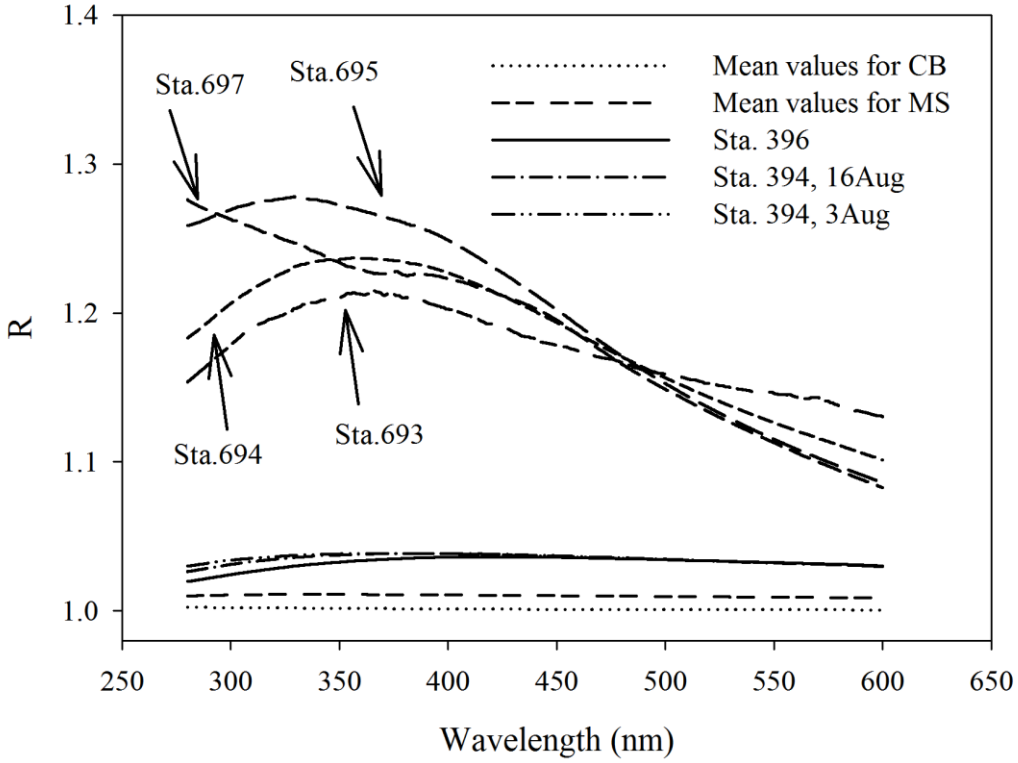

Derivation of the absorption coefficient of minerals. Following the method of Moate et al. (2012), the mass-specific absorption coefficient of suspended minerals, a_M^* (m^2 g^{-1}), for the estuarine transect samples was derived by the regression of the non-algal particulate absorption coefficient (a_{nap}) against the concentration of suspended minerals, M (g m^{-3}), in the form of

$$a_{nap,\lambda} = a_{0,\lambda} + a_M^* \times M$$

where a_0 (m^{-1}) represents the organic particle absorption not removed by the methanol treatment. M was calculated as the difference between the total suspended particulate matter (SPM) and the particulate organic matter (POM). POM was estimated as 2.6 times the particulate organic carbon (POC) (Copin-Montégut, 1980; Martin et al., 1993). The a_{nap}, SPM, and POC data, separately collected by Doxaran et al. (2012) from the SGTs during the same cruise, were used to perform the regression of a_{nap} on M (since our own study did not measure SPM and POC). The regression result for wavelength at 330 nm is shown in Fig. S5A and the derived a_M^* (and a_0) as a function of wavelength are shown in Fig. S5B. The mineral absorption coefficients for the salinity transect samples can thus be calculated as $a_M^* \times M$. The spectral shape and values of a_M^* obtained in the present study are comparable to those in the Conwy and Mersey estuaries of the Irish Sea (Moate et al., 2012). They also mimic the a_M^* spectra of Saharan dusts in red rain collected at the Mediterranean coast in France (Babin and Stramski, 2004). Because a_{nap} showed no significant relationship to the mineral concentration in the shelf and offshore water samples (data not shown), it was not

possible to obtain the a_M^* of these samples from the regression method described above. The upper limits of their mineral absorption coefficients can, however, be estimated as the difference between the total particle absorption coefficient (a_p) and phytoplankton absorption coefficient (a_{phy}).

Fig. S5. Regression of a_{nap} at 330 nm against the mineral cocentration (A) and the derived a_M^* and a_0 (B).

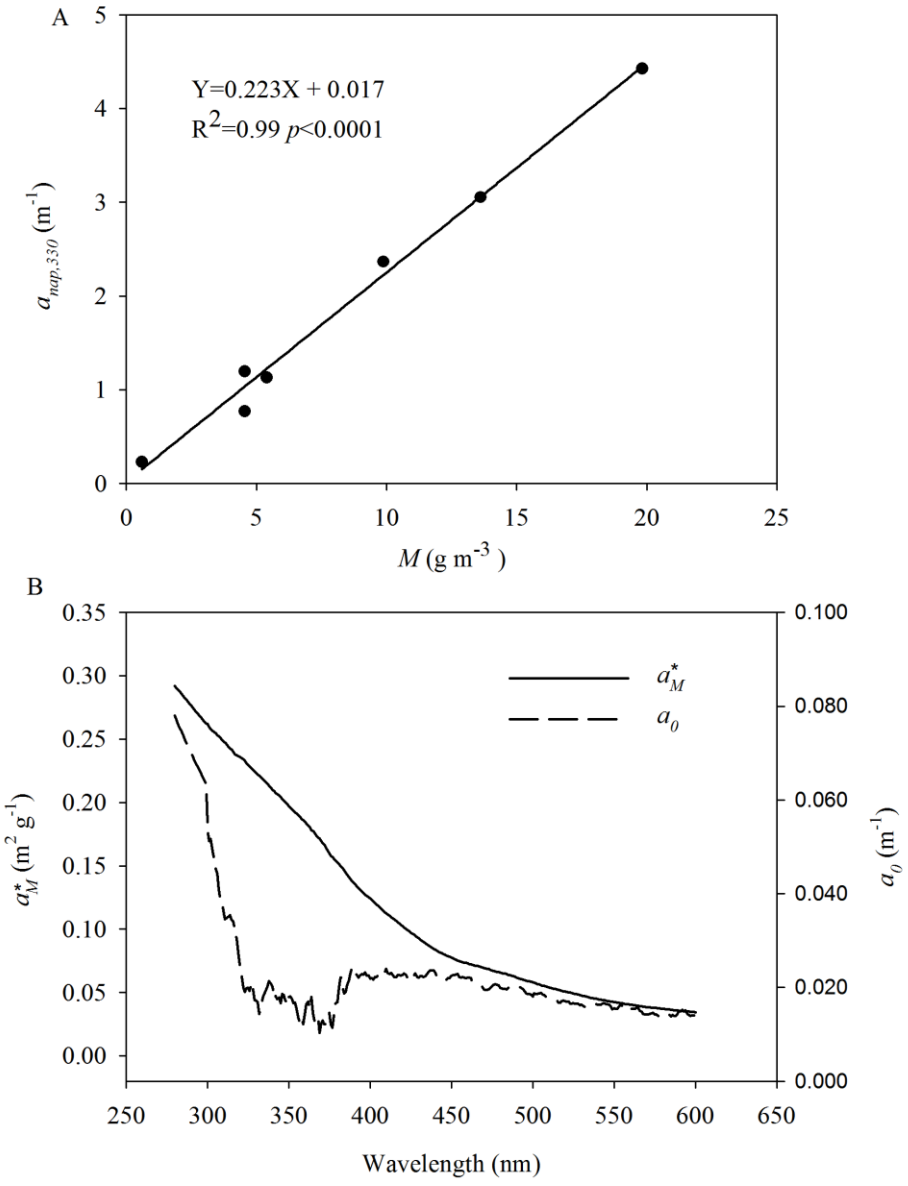

References

Babin, M, and Stramski, D.: Variations in the mass-specific absorption coefficient of mineral particles suspended in water, Limnol. Oceanogr., 49, 756-767, 2004.

Buiteveld, H., Hakvoort, J. M. H., and Donze, M.: The optical properties of pure water, in: SPIE proceeding on ocean optics XII. The Society of Photo-Optical Instrumentation Engineers, edited by: Jaffe, J. S., 174-183, 1994.

Doxaran, D., Ehn, J., Bélanger, S., Matsuoka, A., Hooker, S., and Babin, M.: Optical characterization of suspended particles in the Mackenzie River plume (Canadian Arctic Ocean) and implications for ocean colour remote sensing, Biogeosciences, 9, 3213-3229, 2012.

Fournier, G., and Forand, J. L.: Analytic phase function for ocean water, Proc. SPIE, 2258, 194–201, 1994.

Leymarie, E. , Doxaran, D., and Babin, M.: Uncertainties associated to measurements of inherent optical properties in natural waters, Applied Optics, 49, 5415-5436, 2010.

Moate, B. D., Bowers, D. G., and Thomas, D. N.: Measurements of mineral particle optical absorption properties in turbid estuaries: Intercomparison of methods and implications for optical inversions, Estuarine, Coastal and Shelf Science, 99, 95-107, 2012.

Mobley, C. D., Sundman, L. K., and Boss, E., Phase function effects on oceanic light fields, Appl. Opt., 41, 1035–1050, 2002.

Morel, A: Optical properties of pure water and pure seawater, in Optical Aspects of Oceanography, edited by Jerlov N. G., and Nielsen, E. S., Academic, 1–24., 1974.

Zhang, Y., Xie, H., and Chen, G.: Factors affecting the efficiency of carbon monoxide photoproduction in the St. Lawrence Estuarine system (Canada), Environ. Sci. Technol., 40, 7771-7777, 2006.

Ziolkowski, L. A., and Miller W. L.: Variability of the apparent quantum efficiency of CO photoproduction in the Gulf of Maine and Northwest Atlantic, Mar. Chem., 105, 258-270, 2007.